

Operational Difficulties
Associated with Convective Wet Downbursts

JAY TROBEC
KELO-TV, Sioux Falls, SD

Corresponding author address: Jay Trobec, KELO-TV, 501 South Phillips Avenue, Sioux Falls, SD 57104. E-mail: jtrobec@keloland.com

Abstract

To the operational forecaster, the convective wet downburst is one of the most difficult severe weather threats to predict in real time. Tornadogenesis (or at least supercell development) and hail formation can both be recognized by timely scrutiny of radar volume scans with ample lead time for a “call to action”. But by the time a thunderstorm downburst is detected through remote sensing of a parent thunderstorm by velocity or reflectivity signatures on the WSR-88D or other radar, there is little time to disseminate an effective warning to the public – even when the radar operator is exceptionally vigilant.

Because rapid decision-making is dependent on preexisting conditions, situational awareness of conditions favorable for downbursts is key to maximizing rapid diagnosis of downburst occurrence. Scientifically-established precursors will be weighed for usefulness in operational settings where downburst recognition is required.

1. Introduction

Downbursts are areas of strong, often damaging winds produced by convective downdrafts (Glickman, 2000). They are found in accelerated, downward moving air currents within clouds, and result in an outward burst of winds at the surface (Fujita, 1976). Although severe convective wind events occur in temporal scales from minutes to hours, and spatial scales from misoscale to mesoscale (e.g. gust fronts, line echo wave patterns, derechos), we wish to examine short-lived, isolated downburst situations. Even though such downbursts appear to represent a minority of severe wind reports (less than one-third in the northern High Plains, according to Klimowski et al., 2003), they present operational challenges different from their larger, longer-lasting counterparts.

The benchmark of downburst velocity differs between researchers. Fujita (1976) and Fujita and Byers (1977) set the guideline as a downward speed greater than the approximate ascent or descent speed of a jet aircraft at 300 feet (91 m) AGL, or 3.6 m s^{-1} . That threshold was presumably established for studying downbursts as they apply to aviation. With the deployment of the Doppler radar, Wilson et al. (1984) and Knupp (1989) proposed that a downburst exhibit a divergent, differential radial velocity of at least 10 m s^{-1} within a radius of 4 kilometers.

Downbursts pose a particular hazard to transportation, particularly aviation. They can create wind shear resulting in a sudden and unexpected loss of altitude during takeoff and landing actions. Fujita and Caracena (1977) documented three U.S. aviation accidents involving downbursts in 1975 and 1976 alone. Proctor (1988) concluded that microburst

winds played a role in at least eleven civil transport accidents in the United States from 1974 to 1985. Wolfson et al. (1994) reports 21 aircraft accidents from downbursts or thunderstorm outflow in the U.S. between 1975 and 1994.

In his extensive study of the subject, Fujita (1985) further classified downbursts by size: *microbursts* produce damaging winds <4 km diameter wide, *macrobursts* create damaging winds >4 kilometers in diameter. He estimated that microbursts and macrobursts force wind velocities up to 75 m s^{-1} (168 mph) and 60 m s^{-1} (134 mph) respectively, potentially causing damage equivalent to what Fujita classified an F3 tornado. Therefore, downbursts are also a threat to persons and property on the ground because they can inflict tornado-strength damage.

Downbursts can be differentiated from tornadoes by the damage path they create. Since the wind flow diverges from a central point when an individual downburst reaches the surface ([Fig. 1](#)), the damage also spreads out from the point of contact on the ground, resulting in what Fujita described a starburst pattern. One such pattern resulted from a downburst in Oklahoma in 2002 ([Fig. 2](#)).

Downbursts can also be classified due to the characteristics of the precipitation of the thunderstorm that produces them. A dry microburst is associated with <0.25mm of rain or a radar echo <35 dBZ in intensity, while a wet microburst accompanies >0.25 mm of rain or a radar echo >35 dBZ in intensity (Fujita, 1985; Wakimoto, 2001). It should be noted that these guideline reflectivity values pre-date widespread deployment of the WSR-88D radar.

Dry microbursts are dry-climate favored, and tend to occur near virga or in high-based cumulus clouds elevated above a layer of dry air. As described by Krumm (1954), dry downbursts occur when rain falls from a cloud base, cooling at a moist adiabatic lapse rate (resulting in lower temperatures and greater densities at successive elevations) until the water is evaporated. The parcel then continues to sink, recovering some warmth at the dry adiabatic lapse rate, to the surface.

Wet microbursts are temperate or tropical climate-favored, and can occur in ordinary thunderstorm cells or within stronger thunderstorms possibly containing a mesocyclone ([Table 1](#)). Hybrid cases contain characteristics of each. Although they all pose hazards to both land-based property and aviation, it is the so-called wet or moist downburst that is the focus of this paper.

2. Possible mechanisms

Even before Fujita's landmark research, the existence of the wet downburst and its possible causes were acknowledged in the journals. Following the Thunderstorm Project, Byers and Braham (1948) reported that "it is possible for falling rain to 'trigger' a downdraft of cold air that reaches and spreads out over the surface." Since that time, much has been studied and learned about downburst processes.

A) Initiation

Downbursts originate as a downdraft takes place as part of the complex circulation pattern within the thunderstorm. As hydrometeors (water and ice) form and fall, they entrain

adjoining air with them due to friction (Byers and Braham, 1948). The falling particles not only provide mass for downward force, but negative buoyancy that is further increased through sublimation, melting, and evaporation (Srivastava, 1985, Proctor, 1989; Lee et al., 1992).

As described in a conceptual model by Knupp (1989), the downburst often begins in the mid-level of the thunderstorm, 2-5 km AGL, near the flanks of the updraft in a wake region of convergence downshear from the updraft. That is where entrainment of neighboring air reduces positive buoyancy associated with the updraft, allowing precipitation particles to descend ([Fig. 3](#)). Horizontal storm-relative winds carry the precipitation particles into subsaturated air, leading not only to diabatic cooling from the melting of frozen particles, but also further cooling of the air from evaporation and sublimation processes, supporting the sinking process.

In a supercell thunderstorm, the situation may be more complex because the flow pattern and pressure gradients are different. In their seminal paper on supercell evolution, Lemon and Doswell (1979) described two regions of downdraft within the thunderstorm: the forward-flank downdraft (FFD) associated with the falling-precipitation region of the supercell, and the rear-flank downdraft (RFD). While the FFD is necessary for extending the life of the cell, it is the RFD that tends to produce the strongest downward vertical velocities, and therefore that region is favored for promoting downward momentum ([Fig. 4](#)). The most likely locations for microbursts to occur are within the RFD, the radar “hook echo” region, or the precipitation cascade adjacent to the updraft. The pressure gradient in

the latter area, 2-5 hPa directed at a right angle to storm motion in a classic supercell, would be most efficient at providing acceleration to the flow (Lemon, personal communication).

Klemp and Rotunno (1983) also discuss the downdraft near the occlusion point (close to the northernmost “I” in the Lemon and Doswell schematic in [Fig. 4](#)). This downdraft is produced by the pressure perturbation couplet occurring from localized low pressure stemming from the mesocyclone. The combination of the RFD and the occlusion downdraft can produce one continuous area of downward motion. Since any downbursts created in this circumstance are near the suspect region where tornadoes form, the falling shaft of evaporating precipitation may resemble a condensation funnel, and potentially be misidentified as a tornado. An example of this will be presented later in this paper.

While a thunderstorm does not necessarily need to be a supercell to produce a downburst, wet downbursts frequently occur in storms residing in areas of high CAPE, the same type of environment conducive to supercells. But the necessity of a vertical moisture gradient has also been recognized. During the MIST (Microburst and Severe Thunderstorm) field project in Alabama, Atkins and Wakimoto (1991) reported wet microbursts were favored with low-level moisture capped by a midlevel dry layer. In their idealized representation diagram, Caracena and Flueck (1988) specifically identify the entrainment of midlevel dry air to distinguish the wet microburst from the dry microburst ([Fig. 5](#)).

The presence of a midlevel dry layer is also a contributing factor in other severe weather events such as tornadoes and hailstorms. It does not necessarily differentiate the downburst threat from the threat of other forms of severe weather.

B) Velocity of the downburst

Downdrafts can be intensified to downburst velocity through cooperative processes:

Precipitation loading: The weight (mass) of precipitation particles not only initiates downbursts by gravitational force and downward drag, but sustains and accelerates the downdraft of air (Knupp, 1988; Roberts and Wilson, 1989). As precipitation falls downward, so does the neighboring drier (denser) air due to entrainment as it is dragged into the precipitation cascade. In this manner, the sink is enhanced.

The contribution of precipitation loading can be seen through examination of a complete buoyancy expression utilizing modified virtual temperature from Stull (2000). He quantifies the downward force, including thermal, water vapor, and loading effects as

$$\frac{F}{m} = \frac{T_v \text{ parcel} - T_v \text{ environment}}{T_v \text{ environment}} \cdot |g|,$$

in which F/m is the buoyant force of the rain-mixed air in m/s^2 , T_v is a modified virtual temperature of the parcel and the environment, and g is -9.8 m/s^2 , the gravitational acceleration. For employment of this expression, Stull defines virtual temperature as

$$T_v = T \cdot (1 + 0.61 \cdot r - r_L),$$

where T_v is the virtual temperature, T is the temperature of the parcel, r is the water vapor mixing ratio, and r_L is the liquid water mixing ratio. The effect of liquid water loading is expressed in the density represented by the r_L term (grams of liquid water/grams of dry air).

Stronger thunderstorm updrafts produce larger (heavier) precipitation particles, increasing the effect of precipitation loading (Doswell, 2001) due to their mass.

Phase change: Another contributor to downdraft speed in the wet downburst is phase change - the melting, evaporation, and sublimation of falling hydrometeors. Srivastava (1985) and Knupp (1989) and Roberts and Wilson (1989) suggest that small precipitation particles, assuming they do not evaporate completely, are more efficient producers of evaporational cooling because of the amount of surface area that is exposed to the outside air. But frozen-phase particles would also promote thermodynamic downward motion because of their diabatic cooling potential through melting or sublimation, especially at levels below the melting level (Knupp, 1988). In either case, the resultant cooling sustains negative buoyancy. Wakimoto and Bringi (1988) used polarimetric radar data to suggest the melting of frozen condensate is important to the development of strong wet microbursts. Atlas et al. (2004) went a step further, concluding that “only modest size hail in large concentrations that melt aloft can produce wet microbursts.” They also suggest from their studies in the Tropical Rainfall Measuring Mission (TRMM) that a narrow distribution of hail sizes, confining the melting layer and negative buoyancy, will further enhance the microburst.

Without that melting and evaporation, the descending air would warm through

compressional heating at the dry adiabatic rate, according to parcel theory (Srivastava, 1985; Proctor, 1988). Especially in environments with a stable lapse rate, the parcel would quickly lose its negative buoyancy, and therefore its velocity.

Knupp (1989) concluded that even in cases with cooling due to sublimation of graupel, the descending air becomes positively buoyant as it sinks – in his simulation, by 2°C within a ~1200m layer centered at 2.4 km AGL. But this positive buoyancy is countered in a moist boundary layer condition by condensate loading and downward-directed pressure gradient forces, allowing the downward motion to continue.

Vertical pressure perturbation: The vertical pressure gradient inside the storm can be a significant factor promoting downbursts, especially in supercell thunderstorms (Wakimoto, 2001). In their numeric cloud model simulation of a tornadic supercell, Klemp and Rotunno (1983) suggested mesocyclone dynamics and low-level circulations strengthen the downward force of the rear flank downdraft and developing occlusion downdraft. While they downplay the contribution of precipitation loading, Carbone (1983) documented a tornadic supercell case in which hydrometeor loading was evident, and concluded “the relative importance of hydrometeor loading versus dynamically induced mechanisms for downdraft initiation remains unclear.”

Momentum: Just as the updraft in a thunderstorm can overshoot its equilibrium level (EL), it is reasonable to suggest analogously that the strength of the downward momentum may continue the downdraft to the surface even if competing forces decrease or cancel the parcel's negative buoyancy.

But a more prominent contributor of momentum is the mid-level of the thunderstorm itself, more specifically the winds in that region. Horizontal wind momentum into the thunderstorm may be conserved through the downdraft, contributing to the velocity of the air as it reaches the surface (Fujita and Byers, 1977; Pryor, 2005). Pryor suggests this is a more likely contributor to convective downbursts during the cold season, when downbursts are more dependent on forcing from upper level troughs, rapidly-moving cold fronts, or upper level diffluence than they are during the warm season (defined as 1 June-30 September).

Presumably, horizontal momentum carried into the downdraft could produce a slanted or asymmetric downburst at the surface, such as those described by Fujita (1985) and Todey (1990).

Combination of forces: The optimum conditions may occur with a combination of these factors. As pointed out by Ellrod et al. (2000), strong wet microbursts result from the evaporative efficiency of small raindrops combined with a large supply of slowly melting graupel, which sustains the downdraft to low levels. Negative buoyancy within the low-level downdrafts is created by the collective forces of precipitation loading, melting, and evaporation (Knupp, 1989).

Srivastava (1985) used a one-dimensional model to examine vertical velocities, concluding that although both a virtual temperature deficit and water loading are important, evaporation is the dominant force for producing strong downdrafts. He estimated that the weight of a water content of 1 g kg^{-1} is equivalent to a virtual temperature deficit of 0.25°C in

terms of buoyancy, a fraction of the temperature deficit that would be observed if the water then evaporated completely. The cooling from the evaporation of that same 1 g kg⁻¹ of rain results in 8.3 times the forcing that would result from loading alone (Hjelmfelt, 2003). In addition, winds in the mid-troposphere may transfer horizontal momentum to the evaporatively-driven downdraft (Pryor, 2005).

In summary, downbursts occur when rain-cooled air in a convective cloud becomes denser than its surroundings. The colder air sinks, striking the surface and “rolls out” (outflows) from the center point. Following the rules of density and parcel theory:

-The lower the relative humidity in the mid levels, the more intense the downdraft.

-The higher the relative humidity in the lower levels, the more intense the downdraft (due to increased virtual temperature difference between downdraft parcel and the environment (Srivastava, 1985; Proctor, 1989; Wakimoto, 2001)).

-The colder the air drawn into the downdraft, the greater the negative buoyancy and more intense the downdraft.

3. Environmental precursors

Just as there are atmospheric clues that suggest the potential for tornadoes or hail or other warm season significant weather, there are parameters that may provide the operational forecaster with the situational awareness to anticipate wet downburst production. Over time, numerous factors have been suggested by studying wet downburst climatology.

Lapse Rates: Srivastava (1985) examined the 186 downburst cases occurring during

Project JAWS (Joint Airport Weather Studies), 35 of them identified as wet microbursts. He concluded that microbursts occurred most frequently at lapse rates $>8.5 \text{ K km}^{-1}$, indicating that intense downdrafts are favored as the lapse rate approaches dry adiabatic (Fig. 6). But a further examination of the data shows that in the few cases in which the lapse rates were $<8.5 \text{ K km}^{-1}$, radar reflectivities were also $>40 \text{ dBZ}$. Those are situations in which the microburst is probably in a moist environment, so the data suggests there is not an absolute lower bound of lapse rates when it comes to wet microbursts, though high lapse rates are certainly more supportive of both wet and dry microbursts.

CAPE: Large CAPE (Convective Available Potential Energy) values are beneficial for the thunderstorm environments that produce wet microbursts, because high CAPE indicates the ability of the convective system (positive buoyant energy) to lift the precipitation core to the mid-level dry air that eventually promotes strong downward motion. Thunderstorm updraft strength is directly proportional to CAPE (Weisman and Klemp, 1986; Holton, 2004). Large CAPE also contributes to precipitation loading, when the weight of excessive water content within a cloud sustains the downward force. For instance, if a parcel has a liquid water mixing ratio of 1.0 g kg^{-1} , this is roughly equivalent to about 0.3 deg K of negative buoyancy (Doswell, 1994). High CAPE environments, especially those with high precipitable water content, would be those favorable for wet microburst production.

DCAPE: Downdraft Convective Available Potential Energy is a sounding-based parameter intended for estimating the potential strength of rain-cooled downdrafts.

Researchers have studied it as a possible contributor to tornadogenesis (Rasmussen et al., 1994; Gilmore and Wicker, 1996; Edwards and Thompson, 2000). At this point, DCAPE appears to be a less effective predictor of tornadic thunderstorms than other parameters. But the downdraft is by definition a contributor to the downburst.

Different researchers define DCAPE in different ways. Gilmore and Wicker (1996) calculated it by dropping the minimum wet bulb potential temperature in the 700-500 hPa layer pseudo-adiabatically to the surface without entrainment. The area between this line and the ambient temperature is the DCAPE (Fig. 7). During the VORTEX field study, Rasmussen et al. (1994) proposed a starting point at the minimum wet bulb potential temperature (θ_w) level, in theory the driest layer, in order to account for the greatest evaporational cooling. In either case, highest values are achieved by a combination of steep lapse rates in the low levels (below 700 hPa) and a very dry layer in the mid-levels (700 and 500 hPa).

Theoretically, just as CAPE (subject to other factors such as shear and helicity) may be used as an estimate of updraft velocity ($\sqrt{2 \text{ CAPE}}$), so may DCAPE be used as a rough estimate of downdraft speed ($\sqrt{2 \text{ DCAPE}}$).

However, these numeric values need to be viewed with caution because in practice in a moist environment, parcels are contaminated by the entrainment of significant amounts of ambient air from the surrounding environment (Edwards and Thompson, 2000). In order for the maximum theoretical downdraft velocity to be achieved, the downdraft would have to be saturated all the way to the surface (the air parcel strictly following the θ_w line),

something that is not likely to happen. Gilmore and Wicker (1998) conclude DCAPE is not nearly as good an indicator of downdraft strength as CAPE is of the updraft. Although it asserts that DCAPE overestimates downdraft strength by as much as a factor of two, the National Weather Service's severe weather training course (AWOC, 2005A) suggests forecasters examine DCAPE as an indicator of evaporational cooling potential that could support downbursts.

WINDEX values: After the work of Proctor (1988), an attempt was made by McCann (1994) to estimate downburst wind gust velocity based on atmospheric soundings. McCann's empirical formula,

$$WI = 5[H_M R_Q (\Gamma^2 - 30 + Q_L - 2Q_M)]^{0.5},$$

H_M = The height of the melting level in km above the ground.

R_Q = $Q_L / 12$ (Q_L is the mean mixing ratio in the lowest 1km AGL), and cannot be greater than 1

Γ = Lapse rate in degrees Celsius per km from the surface to the melting level

Q_M = Mixing ratio at the melting level

results in WI, a wind index of maximum wind speed in knots. WINDEX is based on studies of both observed and modeled microbursts.

The literature contains varying reports of WINDEX effectiveness. Gordon and Albert (2005) reported that strong microbursts commonly occur when thunderstorm outflow boundaries move into areas of WINDEX maximums. A study in Australia (Geerts, 2001) concluded that WINDEX was a poor predictor of extreme gust strength, because it did not account for the downward transfer of horizontal momentum. Roeder (1999) found anecdotal value in WINDEX, but believed it is unreliable for wet microbursts because it does not account for the downburst's continued acceleration after it reaches the ground.

A [satellite-derived version of WINDEX](#) is currently available in experimental form through NESDIS, the National Environmental Satellite, Data, and Information Service. As with other sounder-based products, it has the advantage of being freshly-updated each hour. But satellite products are not considered as accurate as balloon soundings, and cannot be measured beneath areas of thick cloud cover.

Equivalent potential temperature (θ_e): The presence of dry air in the mid-troposphere has long been recognized for its importance in downburst production. For this reason, a vertical gradient of equivalent potential temperature is a good indicator of this column-relative mid level dry layer. Equivalent potential temperature may be the most widely used indicator of wet downburst potential.

Operationally, the gradient can be represented by the difference between high water vapor air at the surface and dry, lower water vapor air at the midlevels. Following work on the Microburst and Severe Thunderstorm (MIST) project, the θ_e gradient was identified (Atkins and Wakimoto, 1991). Wheeler (1996) proposed the Microburst Day Potential Index,

$$MDPI = \frac{[\text{Max } \theta_e(\text{Sfc} - 850 \text{ mb}) - \text{Min } \theta_e(660 - < 500 \text{ mb})]}{30 \text{ K}},$$

in which the difference between the maximum θ_e at the low levels is compared to the minimum θ_e at the mid levels. If the difference is greater than 30K (a value based on climatology) resulting in an MDPI >1, there is a potential for wet microbursts. It should be noted that this formula was developed in Florida and the 30K constant may be regionally

dependent. Atkins and Wakimoto suggested a 20K difference in θ_e during the MIST project correlated with microburst days, and the difference was less than 13 K on thunderstorm days with no microbursts. In practice, those guidelines seem to work better in the Midwest than the 30 K microburst day threshold proposed by Wheeler. The quantification of regional dependency in the MDPI may present an opportunity for further study.

Model derived θ_e temperatures are easily plotted on a virtual sounding, and can be displayed for the operational forecaster using computer software programs such as [BUFKIT](#) ([Fig. 8](#)). Of course the normal limitations of model data need to be considered when using equivalent potential temperature in this way.

The MDPI does not consider the CAPE necessary for the wet type convective downburst, but the Wet Microburst Severity Index (WMSI) does. The WMSI (Pryor and Ellrod, 2004) is designed primarily for use with GOES sounder data for estimating the wet downburst generation by satellite remote sensing during the warm season. But the concept is based on the inviscid vertical momentum equation (Doswell, 2001), and verifies the importance of both CAPE and θ_e for wet downburst production.

The WMSI algorithm is represented by the expression

$$WMSI = \frac{CAPE \times TeD}{1000},$$

in which TeD refers to the theta-e deficit in the middle troposphere, producing the negative buoyancy due to evaporational cooling. Similar to the MDPI, theta-e deficit is the difference between the θ_e maximum and θ_e minimum. CAPE is estimated in this instance from the

GOES atmospheric profile. Pryor and Ellrod (2005) have found a statistically significant correlation ($r=0.66$ for daytime events) between higher values of the GOES WMSI and the magnitude of observed surface wind gusts. One significant limitation of GOES WMSI is that data cannot be gathered from cloud-covered areas.

There are, of course, significant caveats when relying solely on environmental precursors to forecast wet downbursts: the storms may not initiate, or the features may be displaced or incorrectly estimated by models or satellites. Even if the data are correct, the false alarm ratio would be exceptionally high, because the same environmental characteristics that produce downbursts promote other severe weather such as hail or tornadoes. More information is required.

4. Radar signatures

Although the process that initiates downbursts is not understood completely, it is understood sufficiently to detect downburst onset through remote sensing.

Downbursts are revealed in infrared satellite imagery of thunderstorm cloud tops as regions of sudden warming, either in circular areas embedded within the anvil, or in a wedge shaped area near the upwind portion of the anvil (Ellrod, 1985). But as Fujita (1985) noted, anvil warming is not only a downburst signature but also a potential signature of tornado production. In addition, satellite data, with the possible exception of rapid scan satellite imagery, is not normally processed and received quickly enough to be used in a warning situation. Use of radar appears to be more effective for timely detection.

Fujita and Byers (1977) recognized the usefulness of radar in detecting the formation of a downburst. They looked at radar reflectivity from the top of the thunderstorm and utilized the assumption that fast moving air is drawn into the downburst source region when the overshooting top collapses into the top of the anvil cloud. Horizontal momentum causes the cell to move faster than other portions of the echo, and the result is a radar signature Fujita and Byers called a spearhead echo ([Fig. 9](#)).

In a wet downburst situation, radar reflectivity can be a good indicator of the event in progress, especially if multiple radar tilts are available. During their creation of a Damaging Downburst Prediction and Detection Algorithm (DDPDA) for the WSR-88D, Smith et al. (2004) discovered that the best predictors of downburst formation in weakly sheared environments were mostly reflectivity-based. Specifically they found that in the 20-45 km range from the radar, the most important variables were VIL (vertically integrated liquid - potential for precipitation loading), the severe hail index (SHI - hail adds mass and cooling through melting), the height of the center of mass (MASSHT - since cores seem to begin at higher heights in downburst storms), and the core aspect ratio (ASP, the ratio of cell width to cell depth). The most noteworthy variables in the 45-80 km range were the SHI, VIL and ASP. At this time, the DDPDA has not been deployed operationally within in the NWS.

In the absence of derived products, a descending reflectivity core aloft is one signature of a possible microburst (Roberts and Wilson, 1989), though high reflectivity values also precede other forms of severe weather. They also detected the presence of

reflectivity notches, and suggested the use of increasing radial convergence (within cloud 3-8 km AGL, or near cloud base) in development of a nowcasting procedure to anticipate microburst production.

Wilson et al. (1984) utilized Doppler radar data in an effort to examine wind structure within downbursts during the JAWS project, concluding that radar would be an effective tool in identifying microbursts and potentially warning aircraft of wind shear hazards. They also suggested that such a local radar be able to scan the lowest few hundreds meters of atmosphere, and have a scan rate of approximately two minutes or less. While such rapid scanning is possible for a dedicated airport radar like the TDWR (Terminal Doppler Weather Radar) deployed at major airports, operational volume scan surveillance radars would have difficulty achieving that scanning speed.

With the development of the NEXRAD network of WSR-88D radar, velocity products have emerged as an effective way of detecting downbursts, through Doppler surveillance of air movement within the thunderstorm. Although there are the well-recognized limitations of Doppler radar usage (e.g. beam spreading, beam height, range folding, dealiasing failure), Doppler radar has become an efficient tool to the operational forecaster. That is especially true now that Level 2 NEXRAD data is available, providing 250 m resolution radial velocity range bins in near-real time.

Schmocker et al. (1996) studied Doppler radar precursors of damaging winds, following up on the previous work of Eilts et al. (1996) and Lemon and Parker (1996). The premise is that convergence at the mid-levels often preceded damaging winds, and that the

convergence was detectable on radar as two opposing velocity currents. Schmocker termed the resulting radar signature Mid-Altitude Radial Convergence (MARC). While MARC was intended as an indicator for other convective wind events such as bow echoes and mesoscale convective systems, it can also be applied to downburst production. MARC is closely related to what Lemon and Burgess (1992) termed the Deep Convergence Zone (DCZ), an area of convergence as much as 10 km in depth near the updraft/downdraft interface. While MARC signatures are mostly confined to the mid-levels, where the strongest convergence is generally found, the DCZ can extend to heights up to 40 k ft (12,200 m) AGL (Lemon, personal communication, 2005). In either case, since the converging air has to be evacuated somewhere, most likely in a downward direction, convergence couplets detected at mid-altitude often precede intense downbursts at the surface.

Detection of MARC is subject to the same limitations as other Doppler radar velocity products, among them viewing angle. If air movement is perpendicular to the beam, the velocity registered relative to the radial is zero. For example, in the case of linear storms the MARC signature is most easily detected in storms moving directly toward or away from the radar. Velocities may be underestimated in linear storms moving in directions other than up- or down-radial (Schmocker et al., 1999).

One important note about using velocity data: convergence signatures alone are not confirmation of a downdraft, since horizontal convergence also occurs in updrafts. Support for a downdraft conclusion is obtained by also examining reflectivity data, with collocated

descending reflectivity cores and collapsing echo tops suggesting downdrafts rather than updrafts (Roberts and Wilson, 1989).

Due to storm movement, convergence can be observed most effectively using the WSR-88D's storm relative motion (SRM) product. It can be seen in the base velocity product, although the operator must then manually account for the movement of the radar target. Additionally, Lemon (2005) indicates that storm scale convergence can be detected through high values (broad values) in radar spectrum width (SW) data. While not widely used in radar meteorology, SW is now more readily available to end users through the greater distribution of NEXRAD Level 2 data.

Once a downburst has reached the surface, the diverging outflow can occasionally be detected on Doppler radar. The downburst must be relatively close to the radar, or be very large in size, because the radar beam must intercept the gust front at a low altitude. Such a case occurred in Mitchell, SD on 5 August 2000. No obvious convergence had been discerned on radar preceding the event. But the SRM data from the 0.5 degree tilt from the WSR-88D at Sioux Falls airport revealed the divergence signature. The large downburst contained 80 kt of divergent flow over 3 km ([Fig. 10](#)). The downburst produced an estimated 120 mph (104 kt) surface gust, destroyed apartments and two mobile homes, and injured ten people. The surface damage path was 1 nm x 1.5 nm (1.6 x 2.4 km) in size.

Roberts and Wilson (1989) also suggested that reflectivity notches and radar-detected rotation as possible microburst signatures. But a technical memorandum (NOAA, 1997)

concludes that those signatures are not valid microburst predictors unless a descending reflectivity core and convergence are also present.

In the future, usage of polarimetric radar may improve wet microburst detection even further. At least one preliminary study found some value in detecting the descent of melting hydrometeors leading to the production of a downburst, though no assessment was made of the predictive value (Scharfenberg, 2003).

5. Visual clues

As a downburst descends from the cloud base, it is sometimes visible as it approaches the ground. To an observer, it might appear to be a descending tornado tube, though it would not have the noticeable convergent spin present in a condensation funnel as it stretches to the ground. A downburst near Veblen, SD in 2002 was observed by trained weather spotters. It had a rough cone shape, so they nearly reported it to the NWS as a tornado - even though time lapse videography showed it to be a downburst, with air diverging as it reached the surface ([Fig. 11](#)). A further cause of misidentification is that downbursts can also occur in concert with tornadoes (Forbes and Wakimoto, 1983), cause damage that may be mistaken for tornado damage (Fujita and Wakimoto, 1981), and may even promote tornadogenesis (Abbey et al., 1982).

In the case of an individual microburst, as opposed to microburst lines discussed by Hjelmfelt (1988), the downcurrent winds strike the surface and then roll out in a circular fashion similar to what one would expect when pouring water on a concrete. The leading

edge of the outflow is a ring diverging from the downburst center ([Fig. 12](#)), caused by the interaction of the downburst core with the surface friction layer, resulting in this “sheath of vorticity” (Caracena et al., 1989). The JAWS and Northern Illinois Research on Downbursts (NIMROD) projects both led to the conclusion that an outflow microburst is often, but not always, encircled by a vortex ring (Fujita, 1985).

The vortex ring can often be seen visually in the form of dust, debris, or precipitation droplets pushed upward as in a rotor motion as lighter surface air is undercut by the advancing dense air of the downburst. To an observer, this may resemble a cloud that appears to roll backward in a plowing motion as the vortex ring approaches ([Fig. 13](#)). At first, the dynamics of the spreading, overturning ring will actually increase the winds at the surface before frictional forces slow their speed (Proctor, 1988; Caracena et al., 1989). The reason for the initial acceleration is vortex stretching (Wakimoto, 2001). Wilson et al. (1984) used Doppler radar to estimate that divergent outflow reaches a peak velocity about five minutes after initial divergence is detected at the surface.

The downburst outflow may appear generally symmetrical from a storm relative position, although from a ground-relative perspective, asymmetry can result due to parent storm motion (Hjelmfelt, 1988). That storm motion can also enhance the magnitude of damaging winds at the surface (Orf and Anderson, 1999).

In wet downburst situations, storm chasers in the field who observe the vortex ring from a perpendicular direction can see the entrained rainfall cascade flare out under the

dominance of strong outflow. They call it a “rain foot”, and it helps distinguish the microburst from what might look like a tornado vortex from great distance ([Fig. 14](#)).

While these visual clues help discern what processes are at work in a thunderstorm, they are of only limited value for warning the public. By the time the parcel has transitioned from downburst to strong horizontal outflow wind, the event has quickly diminished.

6. Temporal scale discussion

To the operational forecaster, downbursts pose a difficult problem. They can roar like tornadoes and twist trees like tornadoes. They can produce winds of tornado velocity. We have examined downburst precursors in the environment, and microburst signatures visible with radar and the naked eye. But wet microbursts still provide a unique challenge to National Weather Service forecasters and broadcast meteorologists: how to warn the public, and do so with an acceptable lead time in which to take action.

By definition, a downburst does not contain the rotational component present in a tornado, although there are demonstrated cases of rotating microbursts (Hjelmfelt, 1987; Proctor, 1988; Rinehart et al., 1995). Instead the downburst fits in the category of a severe thunderstorm, because it can produce winds in excess of 50 kt (58 miles per hour). But with potential wind speeds two or three times greater, the public rarely feels properly warned when a downburst occurs in a region covered by a severe thunderstorm warning. A severe thunderstorm warning is also verified with 0.75 inch (1.9 cm) hail, which is a mere nuisance compared to a gust of thunderstorm wind that may exceed 80 kt.

Downbursts also happen quickly, without the developmental radar warning clues that tornadoes often exhibit in their infancy. In contrast to tornadoes, they tend to have short lifetimes, averaging 13 minutes in JAWS (Hjelmfelt, 1988). So even in the best of circumstances, lead time would be a few minutes maximum. That is not very much time for issuance of a “call to action”.

Doswell (1994) estimated that downdrafts lag the updrafts that produce them by about half a convective time scale (the time needed for a parcel to rise from the LCL to the equilibrium level, or about 20 minutes). If such is the case, the developing stage of a downburst would have to be detected within those ten minutes.

During that window, the convergence of air flowing into the downdraft could presumably be detected by Doppler radar, the MARC signature. But if that were to happen, certain assumptions would have to be made:

- 1) The signature would have to be large enough for the radar to sample. Due to the spreading of the radar beam with distance, and the averaging of the velocities within each range bin (spectrum width), the convergence could be “smoothed out”. If the velocity convergence is oriented orthogonal to the radar beam, the velocities would be under-reported.

- 2) The beam would have to be sampling at the correct altitude at the exact time of the convergence. This situation depends on both the distance from the radar to MARC, and at which VCP (volume coverage pattern) the radar is being operated. The VCP determines at

what elevation the radar is scanning. In the case of a wet downdraft, NWS offices would presumably be operating in VCP 11 (precipitation mode) or the recently enacted VCP 12, which provides more frequent coverage of the lowest tilts of the atmosphere for use in convective situations (Brown, 2005).

In VCP 11, it takes approximately 5.5 minutes for one complete volume scan to be completed, sweeping 14 elevation angles. In VCP 12, the volume scan takes approximately four minutes. In order to detect the convergence signature associated with a downburst, it has been suggested that the radar must be surveilling the 5-11 k ft (1.5-3.4 km) midlevel layer of the troposphere.

During both VCP 11 ([Fig. 15](#)) and VCP 12 ([Fig. 16](#)), the elevation angles intercept that 5-11 k ft (1.5-3.4 km) layer only at distances between approximately 8 km (due to the cone of silence directly above the radar) and 150 km from the radar data acquisition site. The pencil beam has to intercept the convergence at just the right time in order to depict it on the PPI display.

Fujita (1985) defined the average duration of microburst winds as the period of one-half of the peak wind speed. Using that measure, the average half-speed period of wet and dry microbursts is approximately three minutes. In the NIMROD study, Chicago 1978, the downburst cases studied averaged 3.4 minutes in length. In the JAWS study, Denver 1982, the average downburst event averaged 2.8 minutes in length ([Fig. 17](#)).

An examination of the results of Wilson et al. (1984) also suggest three minutes is the

approximate length of the window of opportunity for radar detection. While studying the evolution of the microburst wind field during the JAWS project ([Fig. 18](#)), they concluded that the average downdraft is above two km AGL five minutes before initial surface divergence (*T-5 min.*), and approximately 1 km above the surface two minutes before initial surface divergence (*T-2 min.*). This is the key height and time period for radar detection of the downdraft.

Given the length of time it takes to complete a volume scan on the WSR-88D, it is almost a matter of chance that the downburst is caught at the appropriate surveillance elevation angle, and that the operator is watching that particular tilt on his PPI display, unless he has situational awareness to be anticipating a downburst.

Even with a local warning radar scanning at a single, low-level tilt angle (such as those used by many broadcast television stations), operating at approximately one revolution per minute, the operator would get one or two “slices” showing the downburst couplet.

When such a mid-level couplet ($\Delta V > 50$ kt) is detected, the speed of the downburst would bring it to the surface in a time frame of 0-5 minutes (AWOC, 2005). Even if the radar operator is fortunate enough in radar sampling, and skillfully diligent in interrogating the data, it still takes approximately 1-2 minutes to generate and transmit a warning through National Weather Service channels (Liz Queotone, Warning Decision Training Branch, personal communication). That still leaves the time it takes for electronic dissemination, and the time it takes for broadcasters and other end-users of warning statements to pass the information along to the public - something beyond the control of the forecaster. The task is

daunting at best. The only potential way to effectively warn the public is to maximize lead time by quickly identifying radar cues occurring while anticipating downburst events due to preexisting atmospheric conditions.

Time issues arise for even if the downburst is spotted visually. Visible clues can be used to warn for a developing downburst, provided there are trained weather spotters in the field at the correct location, and they are able to discern what is happening. But the necessity for fast action is evident when one examines the relatively short time it takes for a downburst to reach the ground once the visual clues have been established. For example, on 10 July 2002, a downburst occurred near Leola, SD. A convergence couplet was detected on WSR-88 from Aberdeen, at a beam height of 1.9 km ([Fig. 19](#)). In this case, the inbound and outbound maximums of the convergence couplet are slightly displaced downradial in a counter-clockwise fashion. This suggests the downburst may have been slightly rotating (see Rinehart et al., 1995). The rotation would be a signature of a vertical pressure gradient, especially if vorticity increased with decreasing height (Roberts and Wilson, 1989). In this case, there were no corresponding vertical couplets in the lower radar tilts.

Because conditions were also favorable for tornado production, there were several storm chasers in the area, one of which videotaped the descent of a downburst ([Fig. 20](#)). Once the protruding “bag” of precipitation clears the cloud base, it is visible. But as the time stamped images indicate, it takes just over one minute for the downburst to reach the ground, hardly enough time for a formal warning to be issued. That time, of course, is dependent not only on downburst speed, but also cloud base height.

In the Leola case, a trained television meteorologist out in the field recognized the downburst, and his information was broadcast almost immediately because a telephone call was placed directly to his TV station. If there had not been a spotter report, a forecaster might have been hesitant to issue a warning based solely on the radar convergence signature. The sounding from nearby KABR ([Fig. 21](#)) shows the theta-e deficit was marginal at just 21 K, resulting in a MDPI of only 0.7. But DCAPE was high, still suggesting the need for vigilance.

7. Case study – Huron, SD

On 28 August 2002, a wet downburst caused considerable structural damage in Huron SD. The downburst was associated with a supercell that formed over Beadle County, and led to the issuance of a severe thunderstorm warning by the NWS.

Shortly after 1700 CDT, the KABR WSR-88D, located 120 km from Huron, indicated reflectivity returns >50 dBZ north of Huron, consistent with heavy rain or hail production (not shown). Vertically integrated liquid (VIL) was 70 kg m^2 , indicating significant water or ice in the column ([Fig. 22](#)). Given the existing vertical temperature profile, hail production was expected. The VIL dropped rapidly after the storm passed over Huron. The SRM product from the WSR-88D in Aberdeen showed 50 kt of downradial convergence 6.4 km due north of Huron just before the downburst ([Fig. 23](#)). Given the height of the KABR radar beam over Huron, it was likely a MARC couplet in the mid-level of the storm.

The storm produced downburst damage: one-inch hail, a car wash destroyed, downed power lines, and a roof torn off a bowling alley ([Fig. 24](#)). Because there was no tornado warning in effect, patrons of the bowling alley did not seek shelter. Even though they saw the roof above them disappear in the wind, no one was injured. Since the storm occurred during daylight hours, witnesses saw the storm and there were no reports of any tornado sightings.

8. Case study – Enemy Swim, SD

Downburst damage occurred in northeastern South Dakota early on 23 July 2005. The event was well-anticipated given the preexisting environmental conditions.

An examination of the data from the previous evening showed significant downburst potential, with little in the way of synoptic flow to change the profile overnight. Much of South Dakota was under a large CAPE, large theta-e deficit profile. The 0000 UTC sounding for Aberdeen showed an exceptionally dry layer of air beginning 2291 m AGL, although very little CAPE ([Fig. 25](#)).

East of ABR, in the NE corner of South Dakota, instability was better and the 700 hPa cap was slightly weaker. The probability of precipitation listed in the National Weather Service zone forecast was listed at only 20%, which was reasonable given those factors.

But if thunderstorms did initiate, the 0000 UTC WMSI algorithm over most of eastern South Dakota showed high potential for wet microbursts over northeast South Dakota and west central Minnesota ([Fig. 26](#)). The satellite-derived algorithm can only be calculated over cloud-free areas, which meant the area of highest DCAPE was also where the WMSI calculations were most sparse.

Thunderstorms did develop in northeast South Dakota during the early morning. A strong convergence signature, sometimes called a storm velocity convergence (SVC) signature if it comes from the SRM product of the WSR-88D, was detected near Enemy Swim by the KABR WSR-88D at 1206 UTC ([Fig. 27](#)). The peak to peak differential was 80

kt at approximately 3.4 km (11,000 ft) AGL, although it should be noted that the couplet was separated by a blank data gate.

The base reflectivity data from 1210 UTC ([Fig. 28](#)) returned 45 dBZ from the 0.5 degree tilt over the same region, approximately 1.8 km (6,000 ft) AGL. This was about the time the reflectivity core was approaching the surface. Higher tilts of the same radar (not shown) showed reflectivity over the same area to 50 dBZ, thus satisfying criteria suggested in a NOAA technical attachment (Falk, 1998) for issuing a severe thunderstorm warning for a downburst, specifically: (1) High reflectivity core of 50 dBZ to heights of 25,000 ft (7620 m) AGL, along with (2) Storm velocity convergence (SVC) of 50 kt somewhere in the layer 5000 - 11,000 ft (1.5-3.4 km) AGL in or near the high reflectivity core. By the time of the next radar scan at that level, approximately five minutes later, the convergence region had sheared out.

Three storm reports were filed with the Storm Prediction Center for Day and Marshall counties in northeast South Dakota, with estimated winds of 60-80 mph (52-70 kt). One of the damage reports occurred at a campground, where an uprooted tree damaged a trailer and its root system lifted a passenger van ([Fig. 29](#)), although there were no reports of injuries. No evidence of a tornado was presented to the National Weather Service in Aberdeen (Ken Harding, NWS-ABR, personal communication). Yet multiple witnesses interviewed on television (KELO-TV) insisted the damage had to be caused by a tornado, citing the roar created by the strong winds. They were not satisfied that a thunderstorm warning gave them the advance notice of the damaging winds to come.

9. Conclusion

In both of the cases presented, severe thunderstorm warnings were correctly issued by the local NWS office. But those warnings might also have been issued simply due to the presence of hail in those thunderstorms. The words “Severe Thunderstorm Warning” make no distinction between hail and wind events, although the damage created is significantly different.

Given the short duration of downburst events, it is extremely difficult to get a downburst warning to the public. The best chance is probably if a broadcaster is personally watching the radar and sees the velocity pattern developing while they are on the air. The next best chance is if the downburst is witnessed and reported by spotters, though lead time is even smaller since the downburst is already below cloud level.

In either case, the only chance to warn the public occurs when the operational forecaster is anticipating wet downburst production due to preexisting environmental conditions. Additionally, valuable seconds may be gained by future technological improvement of radar algorithms (e.g. Wilson et al., 1984; Dance and Potts, 2002; Smith et al., 2004) that automate radar interrogation of suspect storms.

AVIATION: For remote sensing of developing and ongoing downburst events, improved probability of detection exists through rapid scanning and spatial coverage. Toward this end, terminal Doppler weather radars (TDWR) have been installed near 45 major US airports to protect aviators against wind shear events during the especially

vulnerable periods of takeoff and landing ([Fig. 30](#)). With a volume scan approximately every minute in fastest mode, the scanning speed of TDWR far exceeds the capability of the existing NEXRAD network. The narrow pencil beam width, 0.55 deg compared to WSR-88D's 1.25 deg, allows higher resolution of targets. Researchers have developed algorithms and improved technology to help automate TDWR detection of wind shear related to downbursts (Wolfson et al., 1994; Lincoln Laboratory, 2001).

Significant drawbacks to TDWR exist. Because they operate on the 5 cm C-band wavelength, they are subject to attenuation by hydrometeors (AWOC, 2005B). Since large raindrops and hailstones are frequently present during wet downburst events, the TDWR may be hampered during the very storms they are intended to detect. But perhaps the biggest limitation is aerial coverage. Compared to the expanse of the NEXRAD network, the footprint of the TDWR installations is currently sparse except for the population centers in the northeastern and southern US. The Washington DC to New York City corridor, for instance, is covered by six overlapping TDWR (Ferree, 2005).

In addition, TDWR velocities are detectible only to a distance of 90 kilometers. The WSR-88D returns velocity data to a distance of 230 km, so it remains a superior detection tool over large areas despite its much slower scanning strategy.

But for events that happen to occur in close proximity to the radar acquisition site, the capabilities of the TDWR clearly show the greatest future potential for successful and timely detection of wind shear events, including downbursts. The TDWR system boasts it

can detect and warn pilots about microbursts with a probability of detection in excess of 90 percent (Serafin et al., 2000).

BROADCASTERS: In addition, the interests of the public at large would be represented by further education on the part of broadcasters who deliver warnings to the public. While it is not suggested that broadcasters assume warning responsibilities from the National Weather Service, the delivery of severe weather information would be augmented if broadcasters who have “live radars” also have training in the recognition of downbursts.

In many cases, the wet downburst events occur in cells already carrying severe thunderstorm warnings due to the presence of large hail. But if a broadcaster recognizes a downburst and delivers this information over the airwaves, there could at least be a little bit of lead time that severe winds are likely to occur. This lead time is difficult to provide at present due to the inherent nature of the warning generation process, and by the fact that downbursts are already “covered” by the existing definition of a severe thunderstorm warning.

REFERENCES

- Abbey, R.F., T.T. Fujita, and J.R. McDonald, 1982: Meteorological and engineering analysis of the Bossier City, Louisiana, tornado of 3 December 1978. *Preprints*, 12th Conf. Severe Local Storms, San Antonio, TX, Amer. Meteor. Soc., 135-138.
- Atkins, N., and R. Wakimoto, 1991: [Wet microburst activity over the Southeastern United States: Implications for forecasting](#). *Wea. and Forecasting*, **6**, No. 4, 470-482.
- Atlas, D., C. W. Ulbrich, and C. R. Williams, 2004: Physical origin of a wet microburst: Observations and theory. *J. Atmos Sci.*, **61**, 1186-1196.
- AWOC (Advanced Warning Operations Course), 2005A: [Severe Track 3, Lesson 24: Hybrid/Wet Microburst Detection](#). Web based forecaster training from the National Weather Service Warning Decision Training Branch, IC3-VII-A..
- AWOC (Advanced Warning Operations Course), 2005B: [Severe Track 3: Near range tornadogenesis signatures viewed by the TDWR](#). Web based forecaster training from the National Weather Service Warning Decision Training Branch, IC3-III-3, Part 2.
- Brown, R. A., R. M. Steadham, B. A. Flickinger, R. R. Lee, D. Sirmans, and V. T. Wood, 2005: [New WSR-88D volume coverage pattern 12: Results of field tests](#). *Wea. Forecasting*, **20**, 385-393.
- Byers, H. R., and R. R. Braham Jr., 1948: [Thunderstorm structure and circulation](#). *J. Meteor.*, **5**, 71-86.
- Caracena, F. and J. A. Flueck, 1988: "Classifying and forecasting microburst activity in the Denver, Colorado area," *Jnl of Aircraft*, **25** No. 6, 525-530.
- _____, R.L. Holle, and C.A. Doswell III, 1989: [Microbursts: A Handbook for Visual Identification](#), NOAA/ERL, Natl. Severe Storms Lab., Norman, OK.

- Carbone, R.E., 1983: [A severe frontal rainband. Part II: Tornado parent vortex circulation](#). *J. Atmos. Sci.*, **39**, 2639-2654.
- Dance, S., and Potts, R., 2002: Microburst detection using agent networks. *Journal of Atmospheric and Oceanic Technology*: Vol. 19, No. 5, pp. 646-653.
- Doswell, C.A. III, 1994: Extreme convective windstorms: Current understanding and research. [Report of the proceedings, U.S.-Spain Workshop on Natural Hazards](#) (Barcelona, Spain), National Science Foundation, 44-55.
- _____, 2001: Severe convective storms – an overview. *Severe convective storms*, C.A. Doswell, ed., Amer. Meteor. Soc, 1-26.
- Edwards, R., and R.L. Thompson, 2000: [RUC-2 Supercell Proximity Soundings, Part II: An Independent Assessment of Supercell Forecast Parameters](#). *Preprints*, AMS 20th Conf. Severe Local Storms, Orlando FL.
- Ellrod, G. P., 1985: Dramatic examples of thunderstorm top warming related to downbursts. *Nat. Wea. Assoc. Digest*, **10** :2, 7.
- _____, J. P. Nelson III, M. R. Witiw, L. Bottos, and W. P. Roeder, 2000: Experimental GOES sounder products for the assessment of downburst potential. *Wea. Forecasting*, **15**, 527-542.
- Falk, K., Harrison, L., and J. Elmore, 1998: [Preliminary downburst climatology and warning guidelines from a single cell thunderstorm database](#). NOAA technical attachment SR/SSD 98-31, 8-1-98.
- Ferree, J., 2005: TDWR data into AWIPS. *NOAA Warning Decision Training Branch*, OB5.
- Available online at <http://www.wdtb.noaa.gov/buildTraining/TDWR/TDWR.pdf>.

- Forbes, G.S., and R.M. Wakimoto, 1983: A concentrated outbreak of tornadoes, downbursts, and microbursts, and implications regarding vortex classification. *Mon. Wea. Rev.*, **111**, 220-235.
- Fujita, T. T., 1976: Spearhead echo and downburst near the approach end of a John F. Kennedy Airport runway, New York City, *SMRP Research paper 137*, University of Chicago, Chicago, Illinois.
- _____, 1984: Andrews AFB Microburst: Six minutes after the touchdown of Air Force One. *SMRP Research Paper 205*, University of Chicago, Chicago, Illinois.
- _____, 1985: The Downburst: Microburst and Macrobust, *SMRP Research paper 210*, University of Chicago, Chicago, Illinois.
- _____, and H. R. Byers, 1977: Spearhead echo and downburst in the crash of an airliner. *Mon. Wea. Rev.*, **105**, 129-146.
- _____, and Caracena, F., 1977: An Analysis of Three Weather Related Aircraft Accidents, *Bull. Amer. Meteor. Soc.*, **58**, 1164-1181.
- _____, and R. W. Wakimoto, 1981: Five scales of airflow associated with a series of downbursts on 16 July 1980. *Mon. Wea. Rev.*, **109**, 1438-1456.
- Geerts, B., 2001: [Estimating downburst-related maximum surface wind speeds by means of proximity soundings in New South Wales, Australia](#). *Wea. Forecasting*, **16**, 261-269.
- Gilmore, M. S. and L. J. Wicker, 1996: [The influence of DCAPE on supercell dynamics](#). *Preprints, 18th Conference on Severe Local Storms*, San Francisco, CA, Amer. Meteor. Soc., 723-727.
- _____ and _____, 1998: The influence of midtropospheric dryness on supercell morphology and evolution. *Mon. Wea. Rev.*, **126**, 943-958.

- Glickman, Todd, editor, 2000: *Glossary of Meteorology*, 2nd edition. American Meteorological Society, Boston.
- Gordon, J. D. and D. Albert, 2005 [accessed]: [A comprehensive severe weather forecast checklist and reference guide](#). *NOAA Technical Service Publication*, NWS Central Region, TSP-10.
- Hjelmfelt, M.R., 1988: [Structure and life cycle of microburst outflows observed in Colorado](#). *J. Appl. Meteor.*, **27**, 900-927.
- _____, 2003: [Microbursts and their Numerical Prediction](#). *Preprints*: Harold D. Orville Symposium, Rapid City SD, South Dakota School of Mines and Technology, Rapid City, 51-67.
- Holton, J.R. 1992: *An Introduction to Dynamic Meteorology*, 4th ed., Academic Press, San Diego, CA, 295-296.
- Klemp, J.B., and R. Rotunno, 1983: A study of the tornadic region within a supercell thunderstorm. *J. Atmos. Sci.*, **40**, 359-377.
- Klimowski, B.A., Bunkers, M.J., Hjelmfelt, M.R., and J.N. Covert, 2003: Regional characteristics of severe wind events. *Bull. Amer. Meteor. Soc.*, **84**, 754.
- Knupp, K. R., 1988: Downdrafts within High Plains cumulonimbi. Part II: Dynamics and thermodynamics. *J. Atmos. Sci.*, **45**, 3965–3982.
- _____, 1989: Numerical simulation of low-level downdraft initiation within precipitating cumulonimbi: some preliminary results. *Mon. Wea. Rev.*, **117**, 1517-1529.
- Krumm, W.R., 1954: On the cause of downdrafts from dry thunderstorms over the plateau area of the United States. *Bull. Amer. Meteor. Soc.*, **35**, 122-126.

- Lee, W., R.E. Carbone and R.M. Wakimoto, 1992: [The evolution and structure of a ``bow-echo microburst" event. Part I: The microburst](#), *Mon. Wea. Rev.*, **120**, 2188-2210.
- Lemon, L.R., and C. A. Doswell III, 1979: Severe thunderstorm evolution and mesocyclone structure as related to tornadogenesis. *Mon. Wea. Rev.*, **107**, 1184–1197.
- _____, and D.W. Burgess, 1993: Supercell associated deep convergence zone revealed by a WSR-88D. *Preprints, 26th Conf. on Radar Meteor.*, Norman, Amer. Meteor. Soc., 206-208.
- _____, and S. Parker, 1996: The Lahoma deep convergence zone: its characteristics, and role in storm dynamics and severity. *Preprints, 18th Conf. on Severe Local Storms*, Boston, Amer. Meteor. Soc., 70-75.
- _____, 2005 [accessed]: Operational uses of velocity spectrum width data. *Australian Sky and Weather*, online at <http://www.stormchasers.au.com/lemon13.htm>.
- Lincoln Laboratory, 2001: Terminal Doppler weather radar (TDWR). *Massachusetts Institute of Technology*. Available online at <http://www.ll.mit.edu/AviationWeather/TDRW-flyer.html>, [accessed 2006].
- McCann, D. W., 1994: WINDEX-A new index for forecasting microburst potential. *Wea. and Forecasting*, **9**, 532-541.
- Miller, R.C., 1972: Notes on analysis and severe-storm forecasting procedures of the [Air Force Global Weather Central, Technical report 200 \(revised\)](#), *Air Weather Service, USAF*, Offutt AFB, Nebraska.
- Miller, D., and D. Burgess, 2003: [Terminal Doppler weather radar observations of a microburst](#). *Preprints, 31st Conf. on Radar Met.*, AMS, Seattle, WA., 6-12 August, 2003, 617-620.

- NOAA, 1997: [Techniques for issuing severe thunderstorm and tornado warnings with the WSR-88D Doppler radar](#). Technical memorandum SR-185, 4-97.
- Orf, L. G. and J. R. Anderson, 1999: A numerical study of traveling microbursts. *Mon. Wea. Rev.* **127**, 1244-1257.
- Proctor, F. H., 1988: Numerical simulations of an isolated microburst. Part I: Dynamics and structure. *J. Atmos. Sci.*, **45**, 3137-3160.
- Proctor, F. H., 1989: Numerical simulations of an isolated microburst. Part II: Sensitivity experiments. *J. Atmos. Sci.*, **46**, 2143-2165.
- Pryor, K., and G. Ellrod, 2004: [WMSI – A new index for forecasting wet microburst severity](#). *National Weather Association Electronic Journal of Operational Meteorology*, 2004-EJ3.
- _____, 2005: [GOES WMSI-Progress and developments](#), *Preprints*, 21st Conf. on Wea. Analysis and Forecasting, AMS, Washington, DC, P1.57.
- _____, 2005a [accessed]: The role of downward momentum transport in the generation of convective downbursts. Website of *NESDIS*, online at <http://www.orbit.nesdis.noaa.gov/smcd/opdb/kpryor/mburst/dbpaper.pdf>.
- Rasmussen, E. N., J. M. Straka, R. P. Davies-Jones, C. A. Doswell, F. H. Carr, M. D. Eilts, and D. E. MacGorman, 1994: Verification of the Origins of Rotation in Tornadoes Experiment: VORTEX. *Bull. Amer. Meteor. Soc.*, **75**, 995-1006.
- Rinehart, R. E., Borho, A., and C. Curtiss, 1995: Microburst Rotation: Simulations and Observations. *J. of Applied Meteor.*, **34**, 1267-1285.
- Roberts, R.D., and J.W. Wilson, 1989: A proposed microburst nowcasting procedure using single-Doppler radar. *J. Climate Appl. Meteor.*, **28**, 285–303.

- Roeder, W. P., 1999: [Microburst refresher training](#). *45th Weather Squadron Training Meeting*, Patrick Air Force Base, Florida.
- Scharfenberg, K.A., 2003: [Polarimetric radar signatures in microburst-producing thunderstorms](#). Preprints, *31st Intl. Conf. on Radar Meteor.*, Seattle, WA, Amer. Meteor. Soc., Vol. II, 581-584.
- Schmocker, G.K., R.W. Przybylinski, and Y.J. Lin, 1996: [Forecasting the initial onset of damaging downburst winds associated with a Mesoscale Convective System \(MCS\) using the Mid-Altitude Radial Convergence \(MARC\) signature](#), *Preprints, 15th Conf. on Weather Analysis and Forecasting*, Norfolk VA, Amer. Meteor. Soc., 306-311.
- Schmocker, G.K., R.W. Przybylinski, and T. Funk, 1999: Forecasting the Onset of Damaging Winds Associated with a Squall Line/ Bow Echo Using the Mid-Altitude Altitude Radial Convergence (MARC) Signature, available online at <http://www.crh.noaa.gov/lmk/soo/presentations/MARCSignature2.pdf> [accessed 2006].
- Serafin, R.J. and J.W. Wilson, J. McCarthy, and T.T. Fujita, 2000: Progress in understanding windshear and implications on aviation. In: R.A. Pielke Jr and R.A. Pielke Sr (eds.), *Storms*, Volume II, London: Routledge Press, 237-252.
- Smith, T. M., K. L. Elmore, and S. A. Dulin, 2004: A damaging downburst prediction and detection algorithm for the WSR-88D. *Wea. and Forecasting*. **19**, Amer. Meteor. Soc., 240-250.
- Srivastava, R. C., 1985: A simple model of evaporatively driven downdraft: Application to microburst downdraft. *J. Atmos. Sci.*, **42**, 1004-1023.
- Stull, R. B., 2000: *Meteorology for scientists and engineers*, 2nd ed. Brooks/Cole Thompson Learning, 502 pp.

- Today, D.P., 1990: Further numerical modeling studies of microbursts. M.S. thesis, Dept. of Atmospheric Sciences, South Dakota School of Mines and Technology, 121 pp.
- Wakimoto, R. M., 1985: Forecasting dry microburst activity over the High Plains. *Mon. Wea. Rev.*, **113**, 1131-1143.
- _____, 2001: Convectively driven high wind events. *Severe Convective Storms*, Meteor. Monogr., No. 50, Amer. Meteor. Soc., 255-298.
- _____, and V. N. Bringi, 1988: Dual polarization observations of microbursts associated with intense convection: The 20 July storm during the MIST project. *Mon. Wea. Rev.*, **116**, 1521-1539.
- Weisman, M.L. and J.B. Klemp, 1986: Characteristics of isolated convective storms. *Mesoscale Meteorology and Forecasting*, P.S. Ray, ed., Amer. Meteor. Soc., Boston, 331-358.
- Wheeler, M., 1996: Verification and implementation of Microburst Day Potential (MDPI) and Wind Index (WINDEX) forecasting tools at Cape Canaveral Air Station, *AMU Report*, 24 pp.
- Wilson J.W., R.D. Roberts, C.K. Kessinger and J. McCarthy, 1984: [Microburst wind structure and evaluation of Doppler radar for airport wind shear detection](#), *J. Climate Appl. Meteorol.*, **23**, 898-915.
- Wolfson, M. M., R. L. Delanoy, B. E. Forman, R. G. Hallowell, M. L. Pawlak, and P. D. Smith, 1994: [Automated microburst wind- shear prediction](#). *Lincoln Laboratory Journal*, Vol. 7, MIT, 399-426.

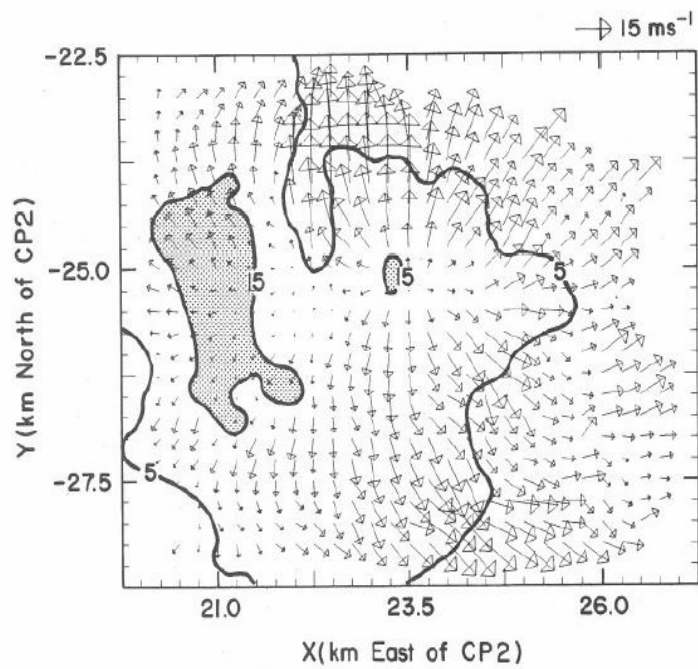


Fig. 1. Reflectivity and horizontal flow field resulting from a microburst at 1445 MDT on 14 July 1982 (Hjelmfelt, 1988).

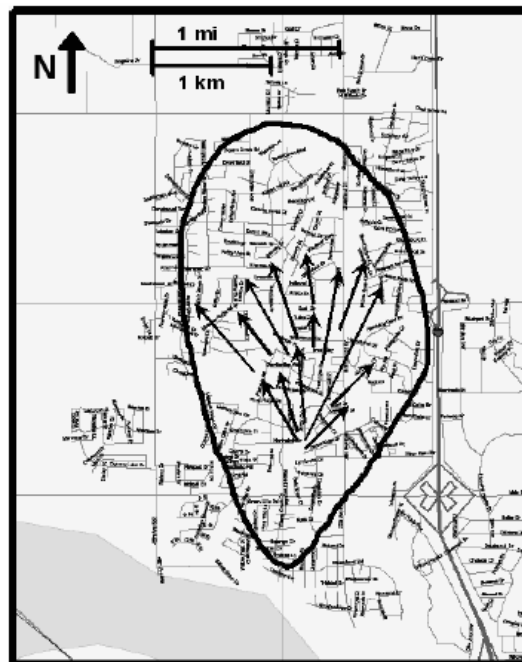


Fig. 2. Starburst damage path resulting from a microburst in Norman, OK on 8 October

2002 (Miller and Burgess, 2003).

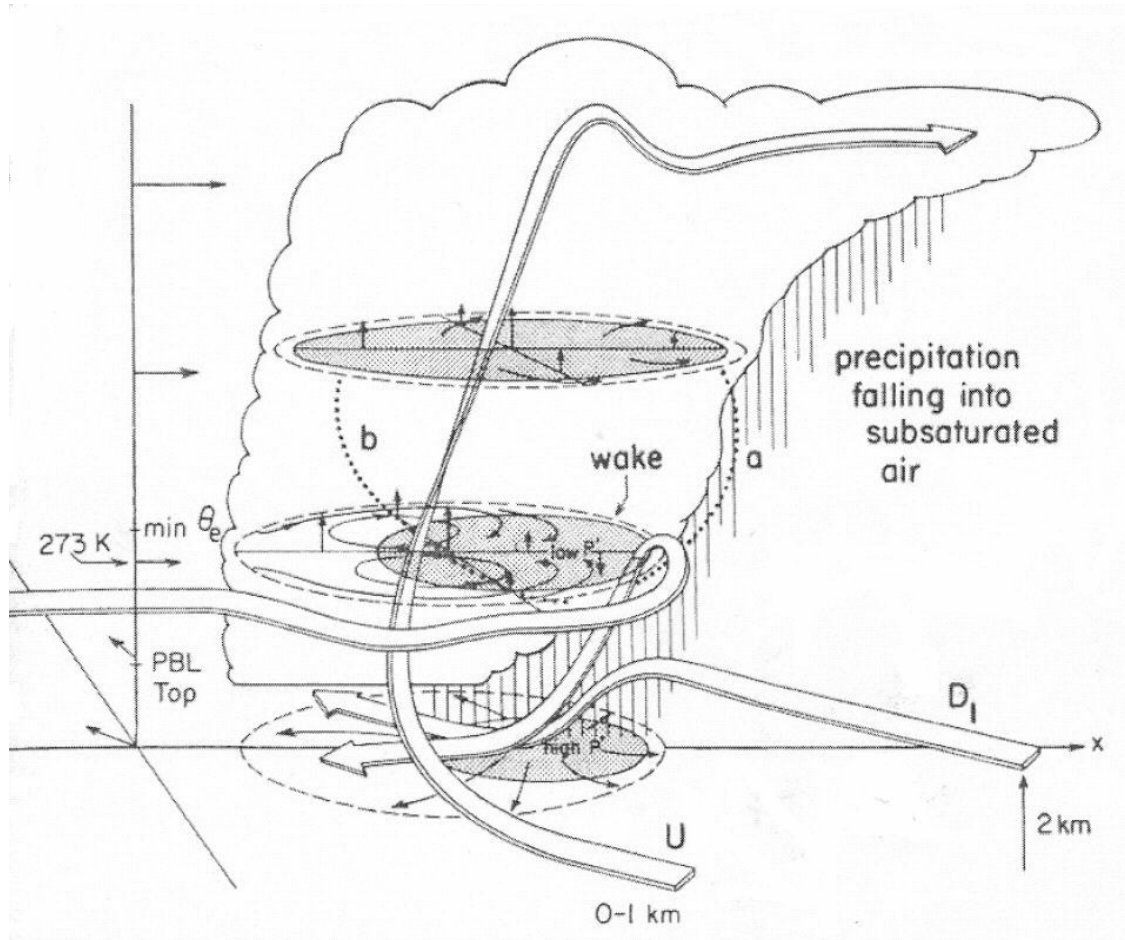


Fig. 3. Plan schematic of conceptual updraft and downdraft motion within a thunderstorm (Knupp, 1989).

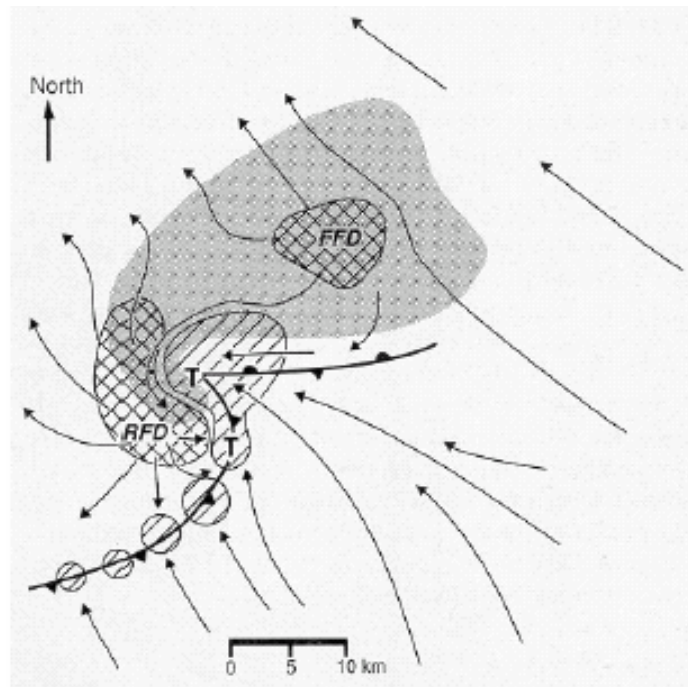


Fig. 4. Plan schematic of a supercell thunderstorm. “T” indicates likely position of a tornado. Adapted from Lemon and Doswell (1979) by Wakimoto (2001).

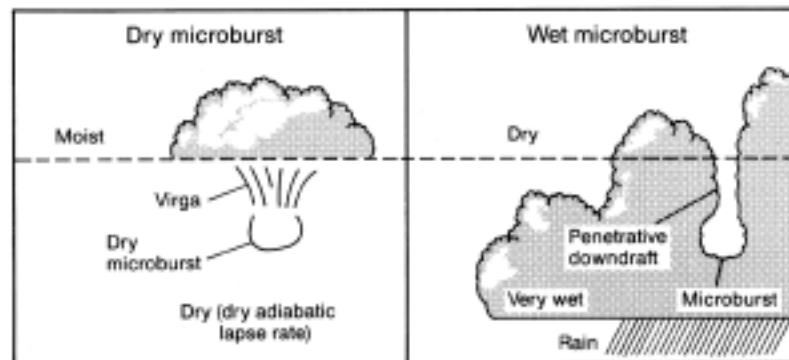


Fig. 5. Conceptual schematic contrasting dry and wet microbursts (Caracena, 1988).

Wet Microburst	Dry Microburst
Moist or temperate climate (humid regions)	Dry climate (arid regions)
Deep nearly saturated layers topped by a dry layer	High cloud bases above a relatively dry subcloud layer (virga)
Cumulonimbus cloud	Cumulonimbus or altocumulus cloud
Large CAPE, BRN, and negative lifted index	Convective temperature must be reached
LCL height low	LCL height near freezing level
Strong radar reflectivity, increasing potential for precipitation loading	Weak radar reflectivity
Strong vertical gradient of equivalent potential temperature	Deep layers of nearly dry adiabatic lapse rates below cloud base
Small or large wet or frozen hydrometeors	Small mostly-frozen hydrometeors

Table 1. General characteristics of wet and dry microbursts, compiled from multiple sources.

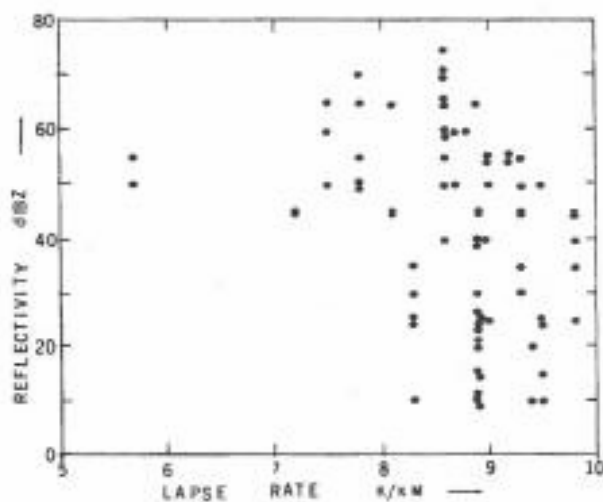
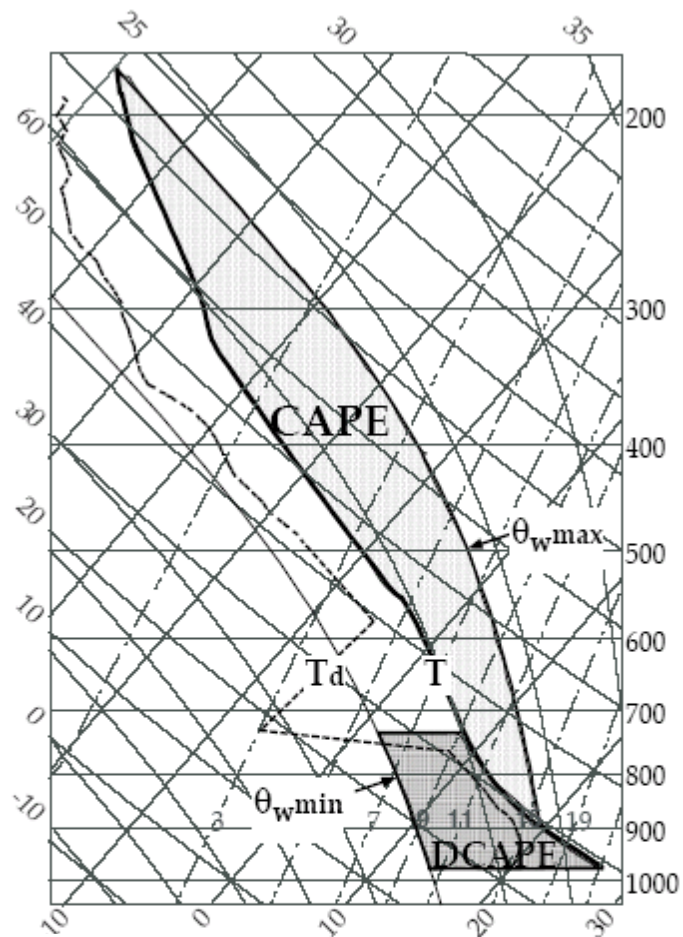


Fig. 6. Microbursts identified during the JAWS Project by radar observations (Srivastava, 1985).



Skew-T diagram illustrating the CAPE (2935 J kg^{-1} ; computed with a parcel of the lowest 1 km mixed boundary layer) for all cases and DCAPE (660 J kg^{-1}) for the 3 g kg^{-1} dry intrusion case. The light shaded area between the temperature profile and ' $\theta_w \text{ max}$ ' (23°C) curve is the CAPE and the darker shaded area between the temperature profile and ' $\theta_w \text{ min}$ ' (15°C) curve is the DCAPE. $\theta_w \text{ min}$ represents the coldest air that could theoretically be brought to the surface in a saturated downdraft. The downdraft parcel used is that which descends from the dry intrusion height (2.3 km).

Fig. 7. Example of a skew-T diagram depicting DCAPE (From Gilmore and Wicker, 1996).

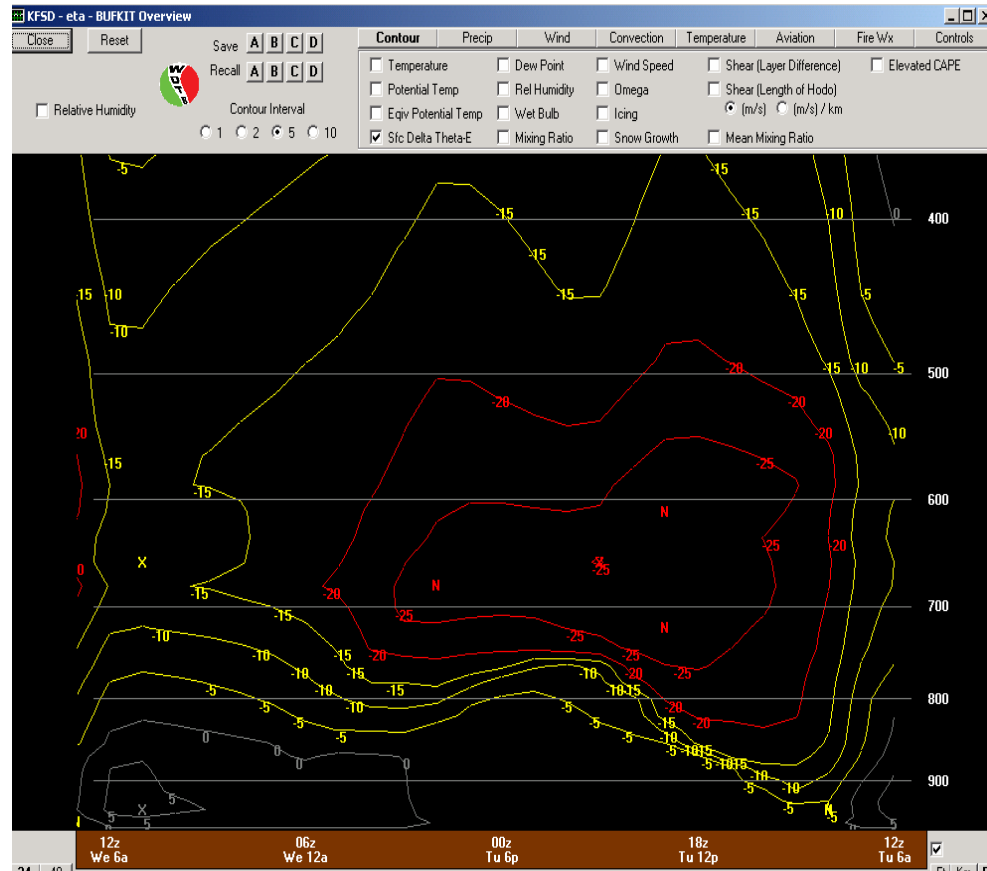


Fig. 8. Typical BUFKIT display showing $\Delta\theta$ -e from the surface to mid-levels. The innermost red circled area depicts the maximum theta deficit, 25 deg K, which is found at the 650 hPa level between 9 am and 9 pm local time.

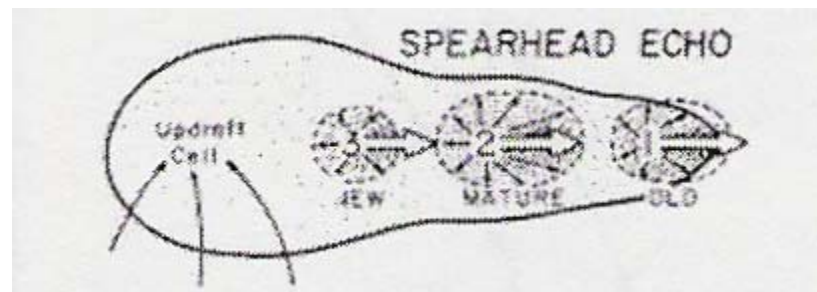


Fig. 9. Diagram of a spearhead echo (Fujita and Byers, 1977). The cell labeled as “new” in the family of downburst cells moves downwind toward the spearhead at a faster rate than the older cells are moving, overtaking them.



Fig. 10. SRM divergence signature, WSR-88D at Sioux Falls (KFSD) on 8 August 2000. Mitchell is 66 nm (106 km) from the RDA.



Fig. 11. Downburst captured on video near Veblen, SD on 10 July 2002 (KELO-TV).

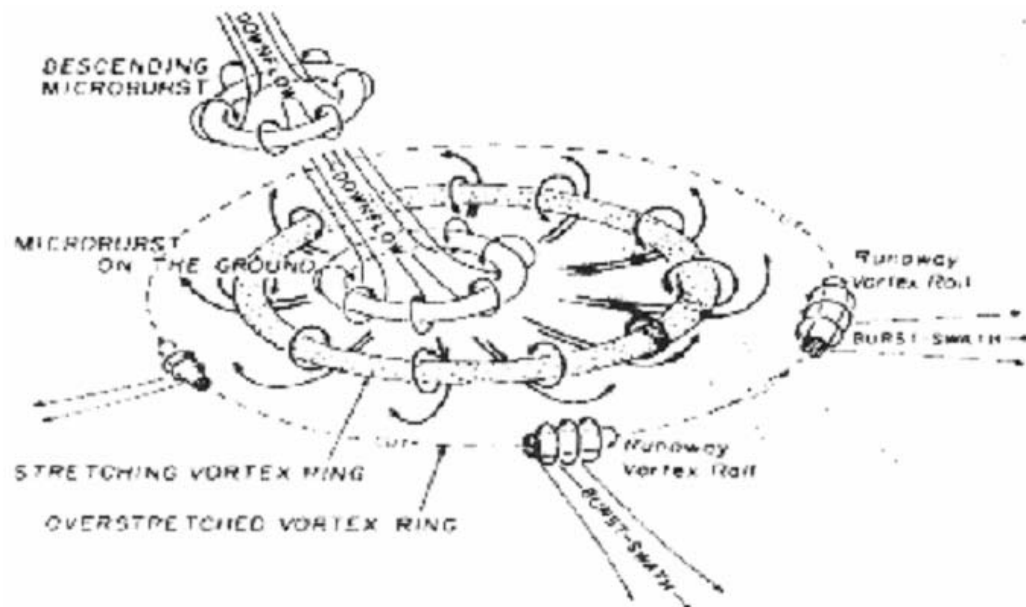


Fig. 12. Schematic plan of a downburst (Fujita, 1984, from vortex ring concept of Caracena).



Fig. 13. Leading edge of a vortex ring as it approaches western Sioux Falls, SD on 12 April 2005. The cloud is rising and curling back toward the divergent center of the outflow (KELO-TV).

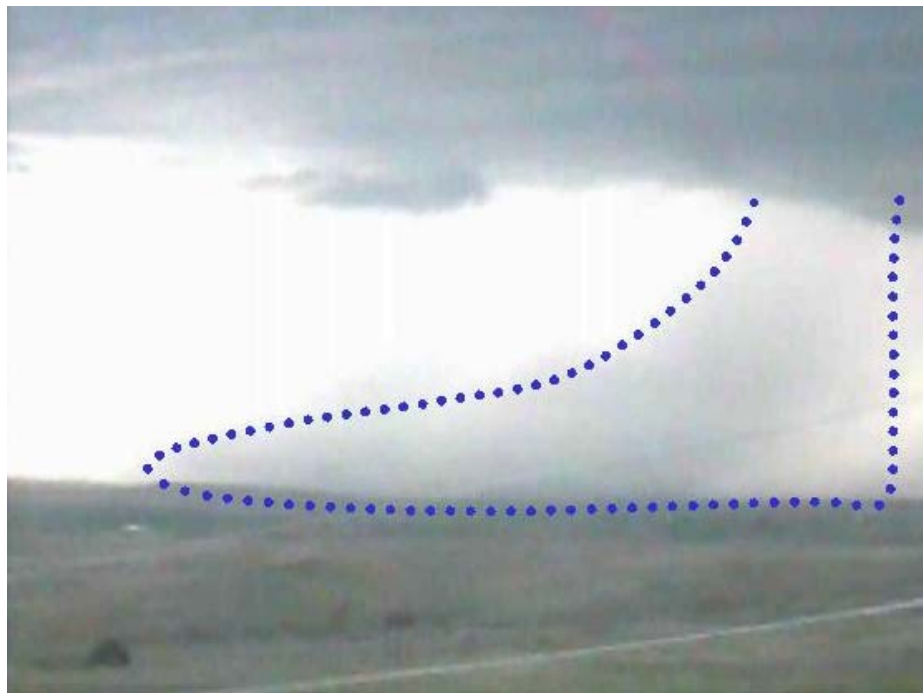


Fig. 14. “Rain foot” (outlined) resulting from a thunderstorm as it approached a mounted video camera in Pierre, SD (KELO-TV).

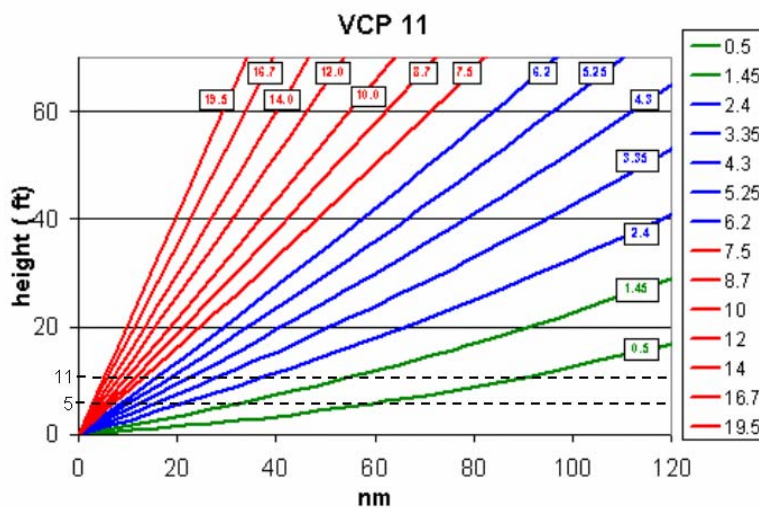


Fig. 15. Elevation angles and beam center height during VCP 11 operation of NEXRAD WSR-88D radar (WDTB). Dashed line depicting 5-11k ft layer added.

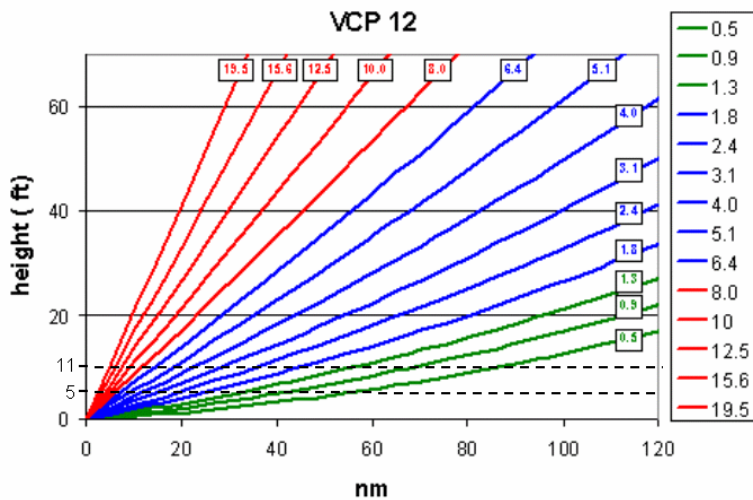


Fig. 16. Elevation angles and beam center height during VCP 12 operation of NEXRAD WSR-88D radar (WDTB). Dashed line depicting 5-11k ft layer added.

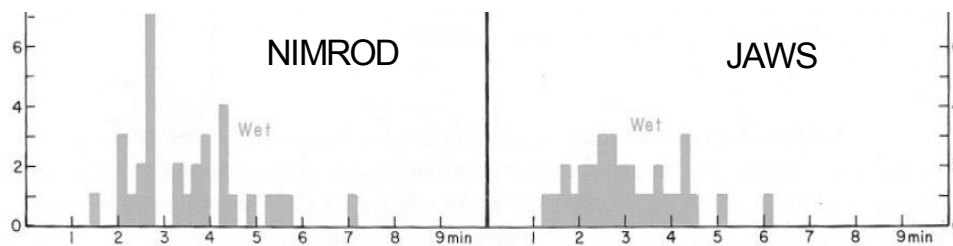


Fig. 17. Duration of wet microbursts in the NIMROD and JAWS projects (adapted from Fujita, 1985).

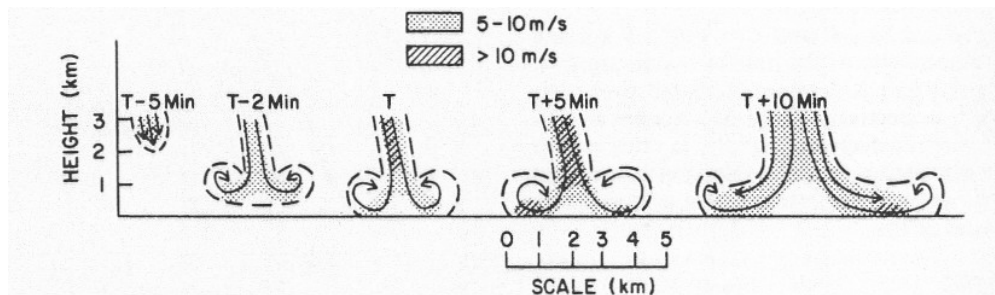


Fig. 18. Vertical cross section of the microburst wind field. T is the time of initial surface divergence. (From Wilson et. al., 1984)



Fig. 19. 0.5 degree base velocity image, 250 m resolution, from KABR WSR-88D on 10 July 2002. Convergence couplet near Leola circled.



Fig. 20. Time sequence showing descent of a downburst near Leola, SD on 10 July 2002. Arrows and elapsed time added (KELO-TV).

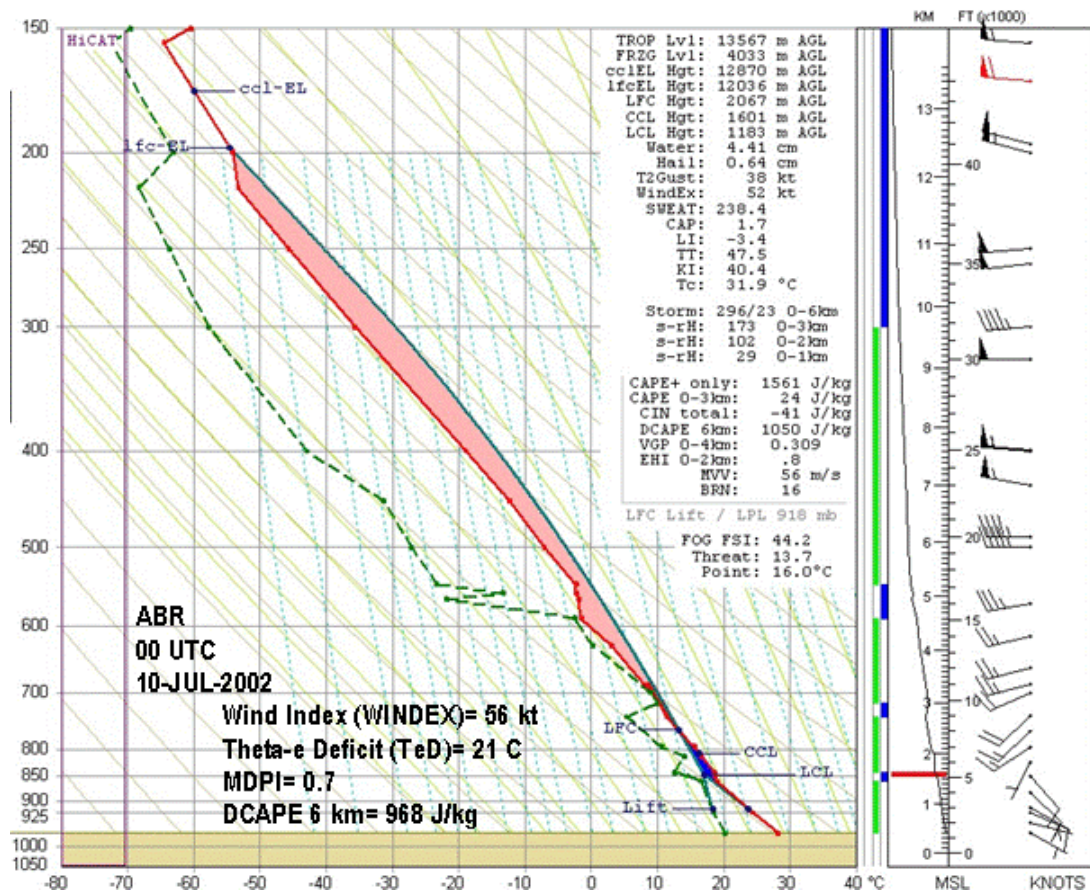


Fig. 21. RAOB sounding for KABR at 0000 UTC on 10 July 2002.

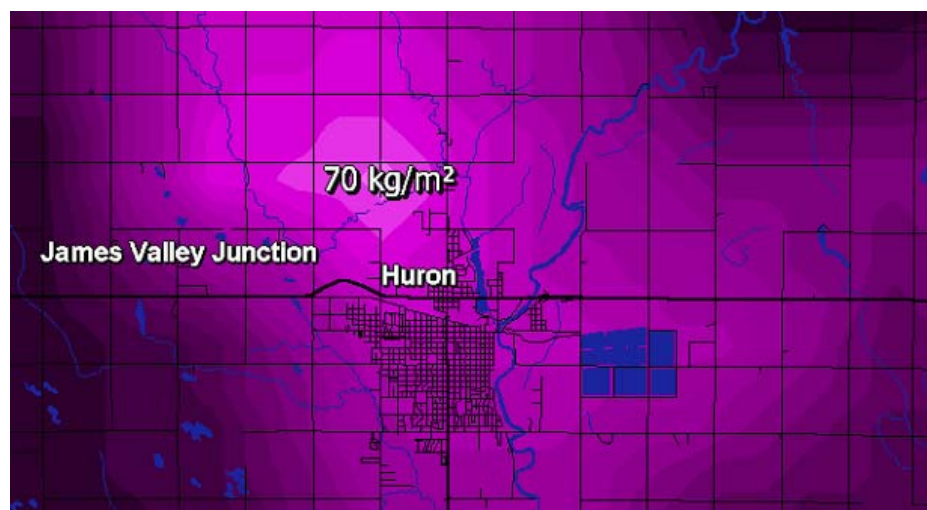


Fig. 22. VIL product from the KABR WSR-88D on 28 August 2002 immediately preceding the downburst. Data smoothing applied. One mi township sections visible.



Fig. 23. SRM product from the KABR WSR-88D on 28 August 2022 immediately preceding the downburst. 50 kt convergence couplet circled.



Fig. 24. Damage in Huron at a car wash (left) and a bowling alley (center and right) following a downburst on 28 August 2022 (KELO-TV).

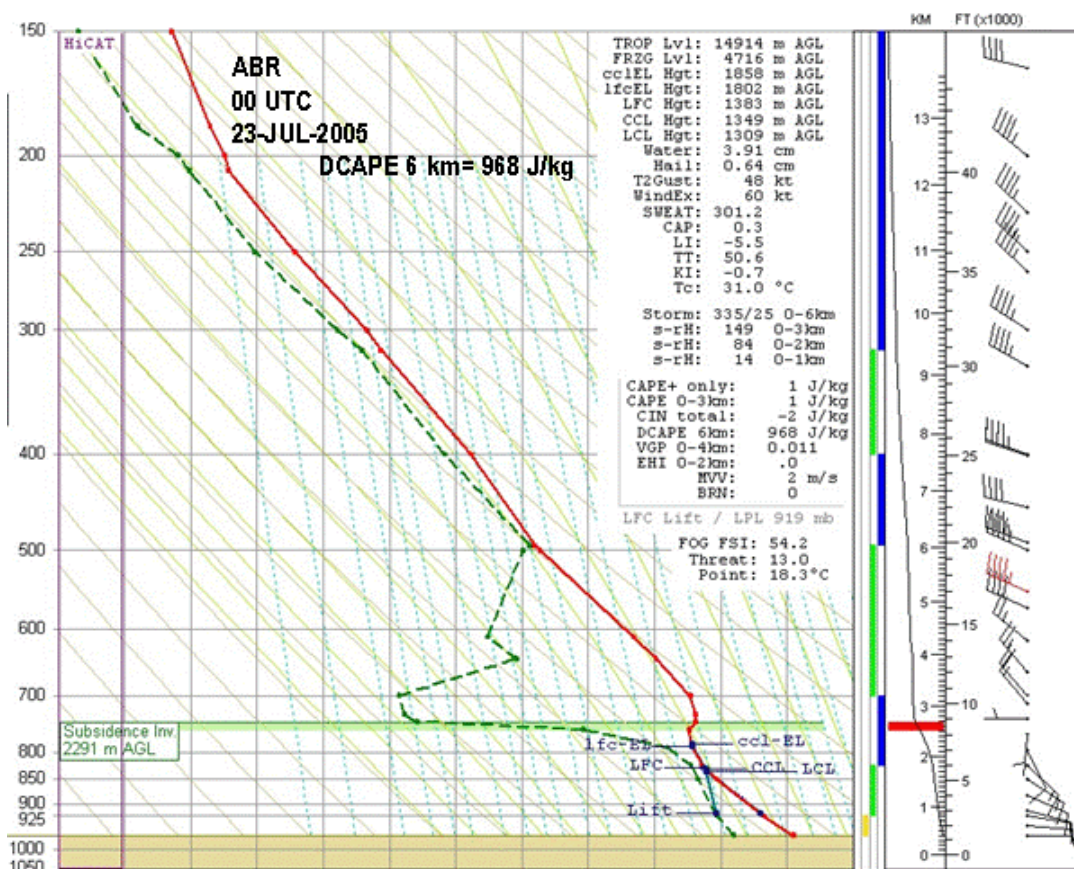


Fig. 25. RAOB sounding from KABR at 0000 UTC on 23 July 2005.

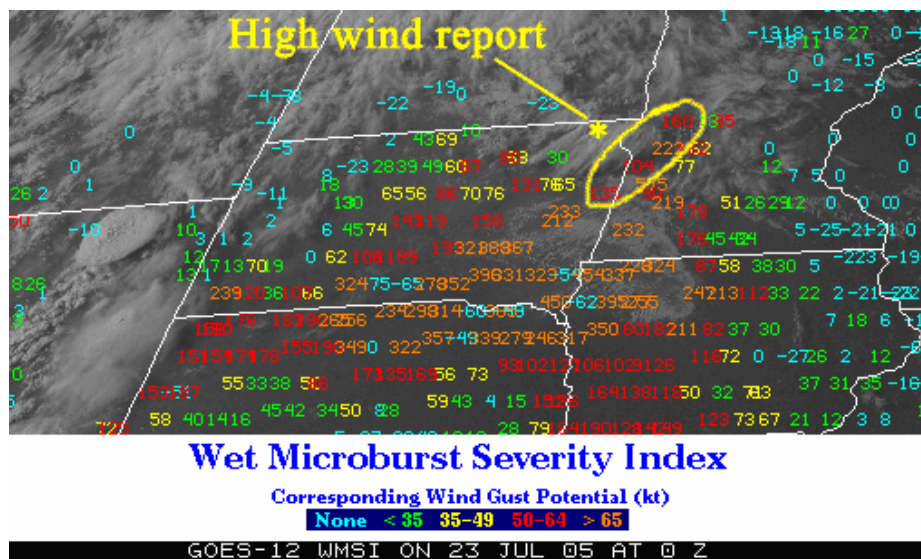


Fig. 26. GOES WMSI imagery from 0000 UTC 23 July 2005. Red numbers indicate potential wind gust of 50-64 kt, and orange numbers >65 kt. Adapted from NESDIS archive, available online at <http://ftp.orbit.nesdis.noaa.gov/pub/smcd/opdb/wmsi/>).

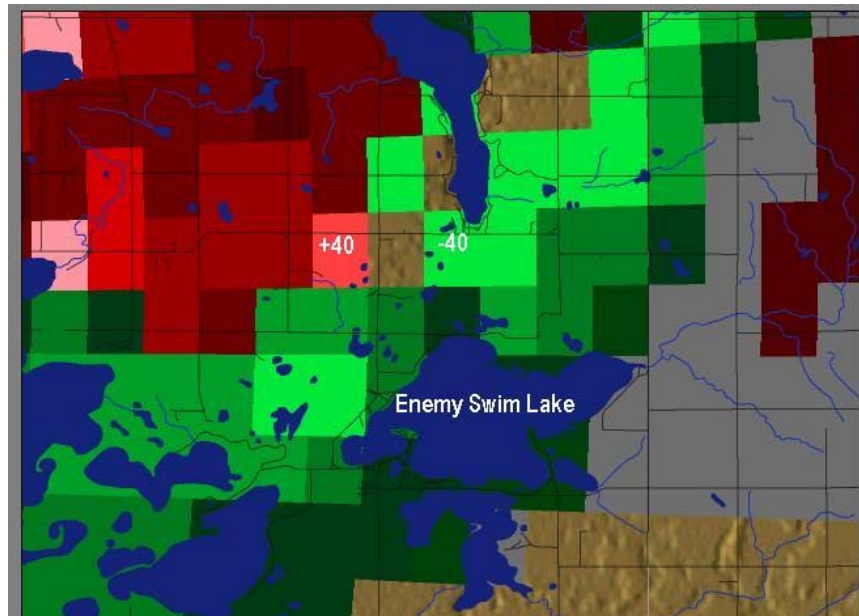


Fig. 27. SRM image at 2.4 degree tilt from KABR WSR-88D, 1206 UTC 23 July 2005. RDA located to the west. Beam height approximately 11 k ft.

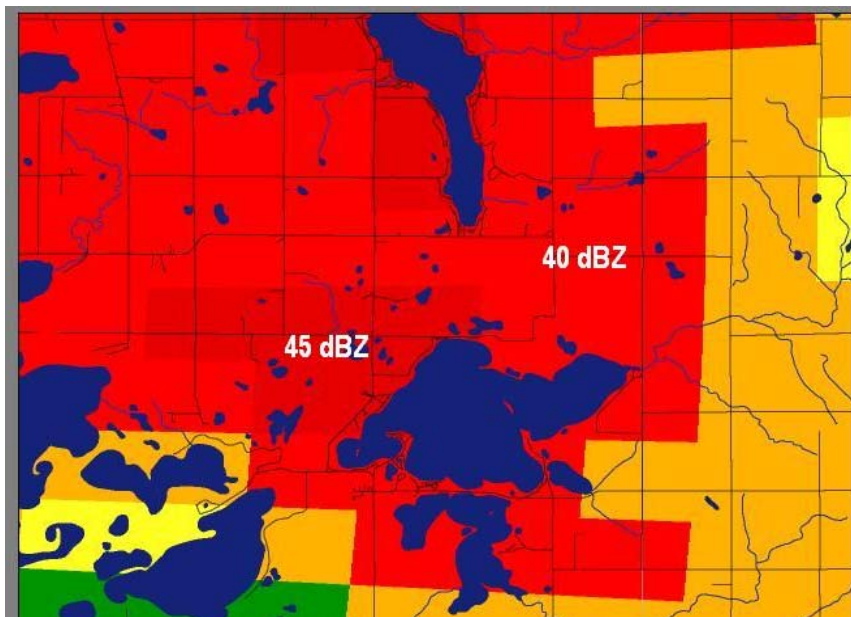


Fig. 28. Base reflectivity at 0.5 degree tilt from KABR WSR-88D, 1210 UTC 23 July 2005. Same view at previous figure.



Fig. 29. Enemy Swim, SD campground on 23 July 2005 after downburst event (KELO-TV).

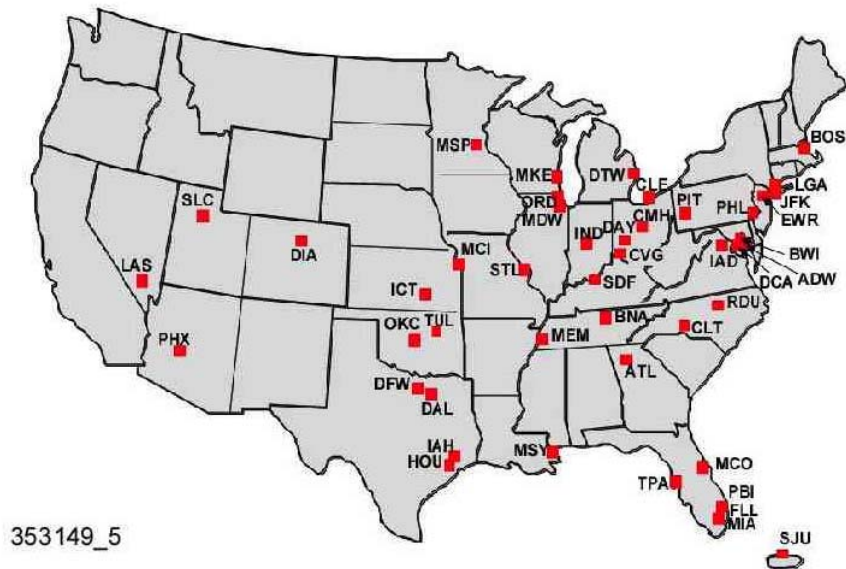


Fig. 29. Map of TDWR installation sites at airports across the US. (From MIT Lincoln Laboratory.)